ECAS 2022

MDPI

Proceeding Paper

COSMO-CLM Russian Arctic Hindcast 1980–2016: Surface Wind Speed Evaluation and Future Perspectives †

Vladimir Platonov * and Aksinia Boiko

Department of Meteorology and Climatology, Faculty of Geography, Lomonosov Moscow State University, Russia; e-mail@e-mail.com
* Correspondence: vplatonov86@gmail.com

† Presented at 5th International Electronic Conference on Atmospheric Sciences, 16–31 July 2022; Available online: https://ecas2022.sciforum.net/.

Abstract: Surface wind speed reproduction by the novel COSMO-CLM Russian Arctic hindcast with ~12 km grid size for a period 1980–2016 was evaluated in this study according to stations and satellite data. Mean wind speed is well reproduced by the hindcast, while the errors relate mainly to cases when the wind speed is overestimated by the model data up to 2 m/s. However, the extreme values (0.95 and 0.999 quantiles) according to the hindcast are underestimated up to −5 … −10 m/s. Evaluation according to the SAR Radarsat-2 high-resolution satellite images including the FSS score revealed the hindcast's capability to reproduce β-mesoscale processes, unlike the γ-scale processes. Just for all 5 m/s threshold exceeding features ~45 km resolution is enough for relevant reproduction by the hindcast. At the same time, the given model grid size (~12 km) is not sufficient to reproduce extreme wind speeds exceeding 20 m/s. Future perspectives of the COSMO-CLM Russian Arctic hindcast include the evaluations of diurnal cycles, wind speed trends, satellite data analysis for other regions of the Russian Arctic; focus on extreme and severe events statistics assessment; quality estimation based on other high-resolution recent datasets.

Keywords: COSMO-CLM Russian Arctic hindcast; Arctic climate change; extreme wind speeds; model evaluation; SAR satellite wind speed; FSS score

Academic Editor: *Anthony Lupo*

Published: 14 July 2022

1. Introduction

The Arctic is one of the most vulnerable to climate change regions in the world. On average, warming in the Arctic occurs two to four times faster than in the entire globe [1]. It is assumed that the cause of this phenomenon lies in a whole complex of physical processes, most of which are closely related to a sharp decrease of sea ice cover [2,3]. At the same time, regional features of the Arctic warming are significantly different and need to be clarified and detailed [4]. Freeing the surface of the Arctic Ocean from sea ice contributes to an increase of extreme winds frequency [5]. Considering the corresponding growing number of severe weather events in the Arctic and the prospects for the development of the Arctic coast and the Northern Sea Route, it becomes necessary to study in detail the observed climate changes in the Russian Arctic, involving climatic information with fine spatial resolution.

Most of the existing hydrometeorological datasets for the Arctic region are either fragmentary (station and expeditionary observations), or has coarse spatial resolution (tens of kilometers—climate datasets, reanalyses, etc.) or limited temporal coverage (satellite data), which does not allow to resolve many dangerous phenomena and to study their statistical characteristics based on long-term timeseries. The novel detailed COSMO-CLM Russian Arctic hindcast covering 1980–2016 period with ~12 km grid size [6] allows to investigate regional Arctic climate changes features in more details including the surface wind speed spatial patterns. However, it is very important to evaluate this dataset according to independent observational data sources, including stations and satellites. Therefore, the main tasks are to reveal its regional advantages and shortcomings, sources of errors, to get estimates of spatial scale sufficient to resolve different severe events.

2. Materials and Methods

2.1. COSMO-CLM Russian Arctic Hindcast

The COSMO-CLM Russian Arctic hindcast, which includes about a hundred different hydrometeorological characteristics at both surface and model levels (50 levels), was created by the long-term regional atmospheric hydrodynamic simulation based on the COSMO-CLM ver. 5.05 model covered the Barents Sea, Kara Sea and Laptev Sea with grid size 0.108° (~12 km) (Figure 1a). The ERA-Interim reanalysis used as initial and boundary conditions in the final experiments' configuration [7], including the spectral nudging technique. Primary assessments of the obtained meteorological data archive showed the adequacy of its reproduction of the main climatological patterns of the average surface wind speeds. At the same time, the details of the distribution of wind speed are manifested in many regions of the Arctic according to the COSMO-CLM Russian Arctic hindcast, which is not reflected in the parental ERA-Interim global dataset [6].

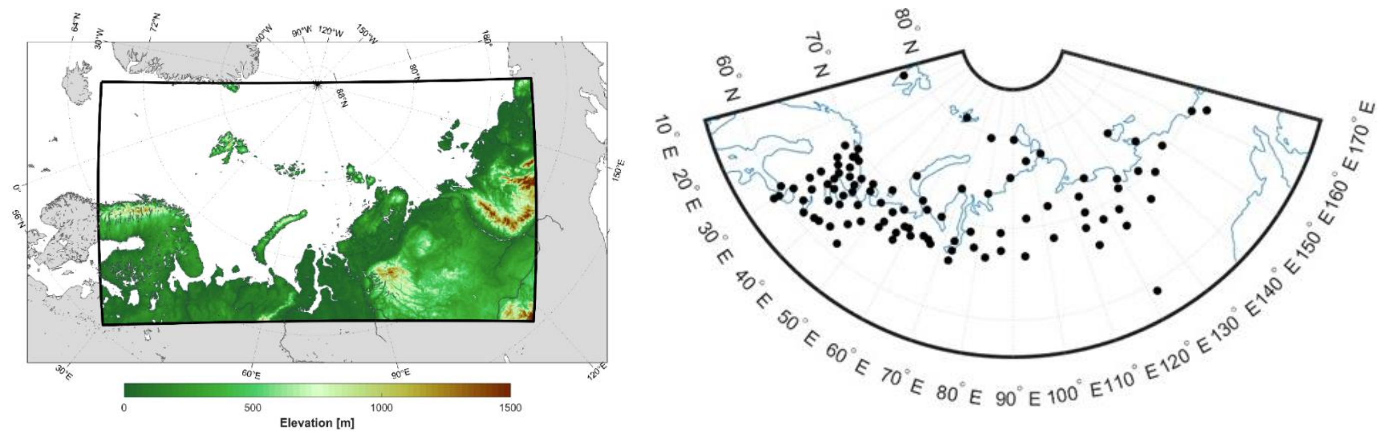

(**a**) (**b**)

Figure 1. COSMO-CLM Russian Arctic hindcast area [6] (**a**) and weather stations location selected in this study (**b**).

Simulations were performed using the shared research facilities of the high-performance computing resources at Lomonosov Moscow State University, supercomputer "Lomonosov-2" [8]. The output step for all variables is 1 h and the total volume of data is about 120 TB. The COSMO-CLM Russian Arctic hindcast data are partially available on the figshare repository for periods 1980–2008 and 2010–2016 [9] and include information on the most important surface fields: 2-m air temperature and humidity, sea level pressure, 10-m wind speed components, surface radiation and turbulence fluxes, and precipitation with 3-hourly timestep. Surface 10-m wind speed components timeseries used in this study. For more detailed information on the hindcast creation and its first evaluations, please see [6,7].

2.2. Weather Stations Data

Weather stations data used to assess the quality of the reproduction of 10-m wind speed, there are data timeseries for 95 stations from the Russian Research Institute for Hydrometeorological Information—World Data Center [10] for a period 1980–2016. All these stations are provided on the Figure 1b. The nearest model grid was selected for each weather station according to their coordinates, taking into account the model land-sea mask. The selected grids used for further comparisons.

2.3. Satellite Data

Synthetic aperture radar (SAR) images from Radarsat-2 satellite used in this study for the area of Novaya Zemlya, since this region is well-known for downslope windstorms development [11] and among the most extreme wind speeds in the Arctic region. The SAR data were downloaded from the NOAA public archive [12]. 19 images with spatial resolution of 2.5 km were selected among all the available images for the period from 2014 to 2016, with the most recognizable structure of the wind speed field and after applying of land and ice masks. Separately, the 2–23 m/s wind speed limits were set manually to eliminate possible errors associated with sea ice surface interpretation. The edges of the image were also cropped since there are observed data distortions along them. Hindcast data having a time difference with a satellite image within 30 min were selected for comparison with satellite data. Then, both model and satellite data were interpolated onto a common regular 5 km grid using the quadratic inverse distance method. Model grid points lacking corresponding satellite data due to the use of different masks were also excluded from the hindcast wind speed data to perform a correct comparison.

2.4. Methods

To compare the selected data sources with the hindcast, the following statistics were calculated: the differences between the hindcast and stations values (or satellite data), then the biases, RMSE and correlation coefficients for these differences representing model errors. The quantiles 0.95, 0.99 and 0.999 were calculated for the stations (or satellite data) and for the corresponding model grid points, as well as the differences between them to study the extreme values of wind speed.

The Fraction Skill Score (FSS) method [13] was applied for spatial comparisons between SAR images and hindcast data. The spatial verification methods allow to estimate the wind speed pattern reproduction in more complete and convenient ways, and to assess spatial resolution required to capture mesoscale features according to different wind speed intervals.

Firstly, the wind speed thresholds were defined as 5, 10, 15 and 20 m/s. For each threshold and data source binary fields were created according to «1» is the value above the given threshold, and «0» is below it. Next, for each grid point in the binary fields the fraction of surrounding points within a given square of length n that have a value of 1 was computed separately for model and satellite data interpolated previously on the common 5 km grid. The corresponding n values were used in this study: 1, 3, 5, 7 and 9 grid cells. In this way, fractions for each square lengths and each wind speed thresholds were calculated, and then the FSS value calculated following formulas (1)–(5):

$$O(n)(i,j) = \frac{1}{n^2}\sum_{k=1}^{n}\sum_{l=1}^{n} I_O\left[i+k-1-\frac{(n-1)}{2}, j+l-1-\frac{(n-1)}{2}\right] \tag{1}$$

$$M(n)(i,j) = \frac{1}{n^2}\sum_{k=1}^{n}\sum_{l=1}^{n} I_M\left[i+k-1-\frac{(n-1)}{2}, j+l-1-\frac{(n-1)}{2}\right] \tag{2}$$

$$MSE(n) = \frac{1}{N_X N_Y}\sum_{i=1}^{N_X}\sum_{j=1}^{N_Y}\left[O_{(n)i,j} - M_{(n)i,j}\right]^2 \tag{3}$$

$$FSS_{(n)} = 1 - \frac{MSE_{(n)}}{MSE_{(n)ref}} \tag{4}$$

$$MSE_{(n)ref} = \frac{1}{N_X N_Y}\left[\sum_{i=1}^{N_X}\sum_{j=1}^{N_Y} O^2{}_{(n)i,j} + \sum_{i=1}^{N_X}\sum_{j=1}^{N_Y} M^2{}_{(n)i,j}\right] \tag{5}$$

Here n—length of square (spatial size), I_O and I_M—binary fields from satellite observations and model data, accordingly, i goes from 1 to N_X and j goes from 1 to N_Y—total number of columns and rows, accordingly.

The FSS value varies from 0 (worst) to 1 (best), FSS > 0.5 indicates a good reproduction [14], applies to estimate an optimal spatial size to reproduce wind speed within different thresholds. The larger the spatial size n, the smoother pattern is reproduced and no detailed structure is captured. However, too small n would be sensitive to features' contours and its displacements, therefore, its edges would be splitter and could not be captured by model. So, the goal of this FSS method is to estimate an optimal spatial size for each wind speed threshold.

3. Results

3.1. Wind Speed Errors

The comparison with the station data showed that the mean wind speed is well reproduced by the COSMO-CLM hindcast, while the errors relate mainly to cases when the wind speed is overestimated by the model data up to 2 m/s. There is also a sufficient number of stations, where the difference between the hindcast and station data is close to zero (Figure 2a). In particular, it is important to note that at three stations with the known highest average wind speeds: Malye Karmakuly, Tiksi and Dikson Island, the average error values really tend to zero. Unlike the average wind speed, the extreme values according to the hindcast are underestimated compared to the stations data with up to −5 m/s for 0.95 quantiles and up to −10 m/s for 0.999 quantiles (Figure 2b).

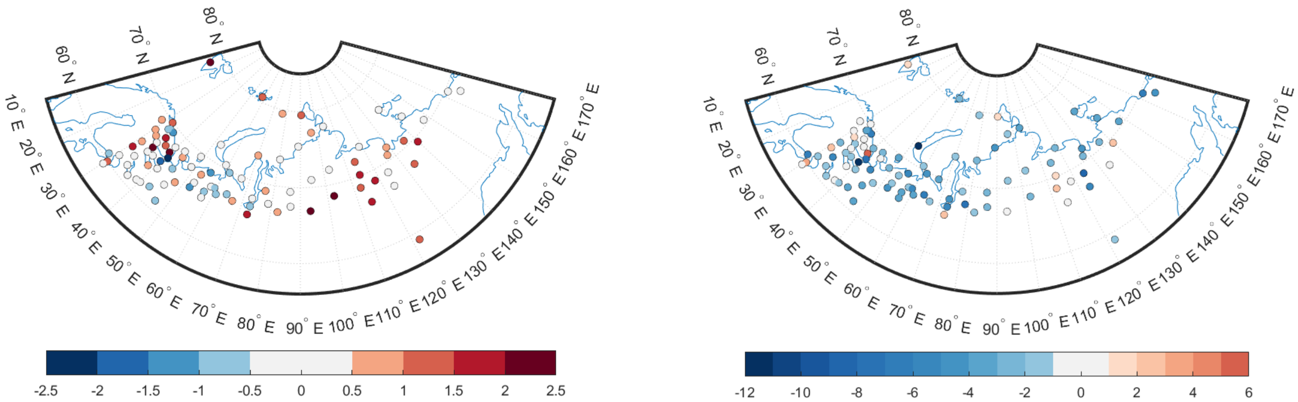

(**a**) (**b**)

Figure 2. Mean errors for hindcast wind speed according to station data (**a**), m/s, difference between hindcast and station data in 0.999 quantiles (**b**), m/s.

3.2. SAR Images Verification Including FSS

SAR images comparison with the hindcast wind speed data showed the moderate wind speed values are often overestimated by model, however differences between the quantiles showed that the more extreme is the observed wind speed, the greater is the probability of underestimation by the model. Model reproduce contour and intensity of the feature well, however its size could be larger than really due to model grid size restrictions. Evaluation of the SAR images according to the FSS score for specific extreme wind speeds cases near the Novaya Zemlya Island showed the hindcast could capture the spatial structure of wind speeds higher than 10 m/s and partially 15 m/s, however could not just reproduce 20 m/s. The FSS analysis revealed the COSMO-CLM Russian Arctic hindcast is successful in 5 m/s features reproduction, because ~45 km is enough resolution (Figure 3). However, the given model resolution (~12 km) is not sufficient to reproduce extreme wind speeds exceeding 15 and 20 m/s, although the 20 m/s threshold has been reproduced by the model for the only one case of 19 (on 7 December 2014).

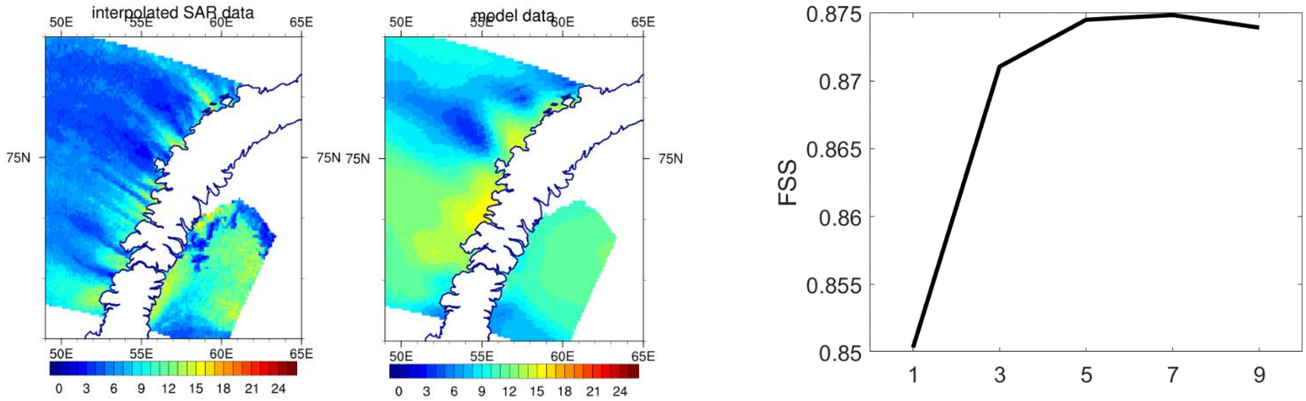

(**a**) (**b**)

Figure 3. SAR (**left**) and hindcast (**right**) wind speed data interpolated on the common grid after applying land and sea ice masks (**a**), m/s; FSS score plot with regard to number of grid points (length *n*) for 5 m/s threshold (**b**) for 28 November 2015 case.

4. Discussion

4.1. Sources of Errors for Wind Speed According to Stations

An additional study for some stations showed that source of the abovementioned errors in surface wind speed could be caused by differences in height and distance between the stations and corresponding model grid points. The examples for wind speed errors include stations Zimnegorsky Mayak and Sosnovets Island with the largest underestimation by the model. Stations situated on the coast or small island, which are not resolved by the model orography interpreting surface as continent. The most stations where the model overestimated wind speed significantly, situated in Siberia. There is another source of errors linked to model orography smoothing over mountain ranges and valleys, which could lead to reproduction of higher wind speeds. The specific future task is to implement any vertical corrections of wind speed to reduce these errors, specifically over the Eastern Siberia mountainous region.

4.2. Discussion of FSS Method Results

Generally, the 5 m/s threshold is reproduced by the hindcast just perfectly with maximal FSS > 0.5. Increasing threshold, the FSS becoming lower and calculating in a smaller number of cases: e.g., for 10 m/s threshold there were 7 cases with FSS > 0.45; 13 cases with FSS = 0 for 15 m/s; only one case with non-zero FSS for 20 m/s with maximal FSS = 0.12. The latter case indicates such features are not captured by model with given spatial sizes, it is beyond the model's possibilities. It is worth to mention that number of grids necessary for successful model reproduction reduces with an increase of wind speed threshold, which is logical to correspond to decrease of spatial scale, when higher wind speeds could be observed. This get the quantitative assessment of spatial scales could be resolved by the COSMO-CLM Russian Arctic hindcast. This result confirmed the model capability to reproduce β-mesoscale processes, unlike the γ-scale processes, which are associated with larger wind speed threshold values.

5. Conclusions

Evaluation of the COSMO-CLM Russian Arctic hindcast showed the average wind speed is well reproduced with slight overestimation mean wind speed. The quantile differences indicated extreme wind speeds underestimation: the error ranges from −2 to −10 m/s for 0.95 and 0.999 quantiles, accordingly.

The FSS analysis against SAR satellite images revealed the hindcast is successful in 5 m/s threshold exceeding features reproduction with ~45 km enough resolution. However, the given model grid size (~12 km) is not sufficient to reproduce extreme wind speeds exceeding 15 and 20 m/s. The number of grids necessary for successful model reproduction reduces with an increase of wind speed threshold, which corresponds to decrease of spatial scale, when higher wind speeds could be observed.

Future perspectives of the COSMO-CLM Russian Arctic hindcast include the evaluations of diurnal cycles, wind speed trends, satellite data for other regions of the Russian Arctic; hindcast prolongation to 2019, sharing more data online; the focus could be on extreme and severe events statistics assessment (downslope windstorms, polar lows climatology using satellite data); quality estimation based on other datasets (e.g., ERA5, CARRA, satellites climatology, etc.).

Author Contributions: Conceptualization, V.P.; methodology, V.P.; validation, V.P. and A.B.; formal analysis, V.P. and A.B.; investigation, V.P.; resources, V.P.; data curation, V.P.; writing—original draft preparation, V.P.; writing—review and editing, V.P.; visualization, A.B.; supervision, V.P.; project administration, V.P.; funding acquisition, V.P. All authors have read and agreed to the published version of the manuscript.

Funding: This research was funded by state project no. AAAA-A16-116032810086-4.

Institutional Review Board Statement: Not applicable.

Informed Consent Statement: Not applicable.

Data Availability Statement: The data presented in this study are openly available in [FigShare] at [https://doi.org/10.6084/m9.figshare.c.5186714], [https://figshare.com/collections/Arctic_COSMO-CLM_reanalysis_all_years/5186714] (accessed on 13 June 2022), reference number [5186714].

Acknowledgments: The research is carried out using the equipment of the Lomonosov Moscow State University shared research facilities “Computational complex for climate modelling and radiation monitoring”.

Conflicts of Interest: The authors declare no conflict of interest.

References

1. Masson-Delmotte, V.; et al. (Eds.) *IPCC, 2021: Climate Change 2021: The Physical Science Basis. Contribution of Working Group I to the Sixth Assessment Report of the Intergovernmental Panel on Climate Change*; Cambridge University Press: Cambridge, UK; New York, NY, USA, 2021; *in press*. https://doi.org/10.1017/9781009157896.
2. Brennan, M.K.; Hakim, G.J.; Blanchard-Wrigglesworth, E. Arctic Sea-Ice Variability During the Instrumental Era. *GRL* **2020**, *47*, 7. https://doi.org/10.1029/2019GL086843
3. Walsh, J.E.; Fetterer, F.; Scott Stewart, J.; Chapman, W.L. A database for depicting Arctic sea ice variations back to 1850. *Geogr. Rev.* **2017**, *107*, 89–107. https://doi.org/10.1111/j.1931-0846.2016.12195.x
4. Maksym, T. Arctic and Antarctic Sea Ice Change: Contrasts, Commonalities, and Causes. *Annu. Rev. Mar. Sci.* **2019**, *11*, 187–213. https://doi.org/10.1146/annurev-marine-010816-060610
5. Moore, G.W.K.; Renfrew I.A. Tip jets and barrier winds: a QuikSCAT climatology of high wind speed events around Greenland. *J. Clim.* **2005**, *18*, 3713–3725. https://doi.org/10.1175/JCLI3455.1
6. Platonov, V.; Varentsov, M. Introducing a New Detailed Long-Term COSMO-CLM Hindcast for the Russian Arctic and the First Results of Its Evaluation. *Atmosphere* **2021**, *12*, 350. http://dx.doi.org/10.3390/atmos12030350
7. Platonov, V.; Varentsov, M. A new detailed long-term hydrometeorological dataset: first results of extreme characteristics estimations for the Russian Arctic seas. *IOP Conf. Ser. Earth Environ. Sci.* **2020**, *611*, 012044. https://doi.org/10.1088/1755-1315/611/1/012044
8. Voevodin, V.; Antonov, A.; Nikitenko, D.; Shvets, P.; Sobolev, S.; Sidorov, I.; Stefanov, K.; Voevodin, V.; Zhumatiy, S. Supercomputer Lomonosov-2: Large Scale, Deep Monitoring and Fine Analytics for the User Community. *Supercomp. Front. Innov.* **2019**, *6*, 4–11. https://doi.org/10.14529/jsfi190201
9. Data from the COSMO-CLM Russian Arctic Hindcast, Figshare. Available online: https://figshare.com/collections/Arctic_COSMO-CLM_reanalysis_all_years/5186714 (accessed on 13 June 2022).
10. Russian Research Institute for Hydrometeorological Information—World Data Center. Available online: http://aisori-m.meteo.ru/ (accessed on 13 June 2022).
11. Shestakova, A.A.; Toropov, P.A.; Matveeva, T.A. Climatology of extreme downslope windstorms in the Russian Arctic. *WACE* **2020**, *28*, 100256. https://doi.org/10.1016/j.wace.2020.100256
12. SAR Radarsat-2 Data. Available online: https://www.ncei.noaa.gov/data/oceans/sar-winds/ (accessed on 13 June 2022).

13. Roberts, N.M.; Lean, H.W. Scale-selective verification of rainfall accumulations from high-resolution forecasts of convective events. *Mon. Weather Rev.* **2008**, *136*, 78–97. https://doi.org/10.1175/2007MWR2123.1
14. Skok, G.; Roberts, N. Analysis of fractions skill score properties for random precipitation fields and ECMWF forecasts. *Quar. J. R. Met. Soc.* **2016**, *142*, 2599–2610. https://doi.org/10.1002/qj.2849